Journal of the Iranian Chemical Society (2020) 17:103–110
https://doi.org/10.1007/s13738-019-01756-6

ORIGINAL PAPER

Synthesis of YTi@Ag nanocomposite and investigation of its structural and antifungal properties

M. Nazeri[1,2] · S. M. Hosseinpour Mashkani[3] · Ramtin Chelongarian[4]

Received: 26 February 2019 / Accepted: 8 August 2019 / Published online: 29 August 2019

Abstract

The aim of the current study is to describe the synthesis, characterization, and measurement of optical and antifungal properties of Yb_2TiO_5@Ag nanocomposites (YTi@Ag) against three standard Candida species including *Candida albicans* (ATCC 1023), *Candida krusei* (ATCC 6258), and *Candida tropicalis* (ATCC 750). YTi@Ag nanocomposites were synthesized through the sol-gel assistant ultrasonic method in an aqueous solution. The antifungal abilities were performed base on macrodilution method as recommended by the Clinical and Laboratory Standards Institute (CLSI, document M27-A3). SEM, XRD, EDX, and FT-IR were applied to characterize structural and morphological characteristics of nanocomposites. In addition, several antifungal tests were performed to investigate the impact of YTi@Ag nanocomposites on the Candida species. Minimum inhibitory concentration (MIC^{50}) measurements of the YTi@Ag NPs against *C. albicans* (ATCC 1023), *C. krusei* (ATCC 6258), and *C. tropicalis* (ATCC 750) after 24 and 48 h were 4 and 32 µg/ml, respectively. MIC^{50} results show that as-synthesized YTi@Ag nanocomposites are efficient as an alternative antibacterial/antifungal agent. The band gap of bare Yb_2TiO_5 and YTi@Ag nanocomposites is 3 and 2.85 eV, respectively. Ag-doped Yb_2TiO_5 has advantage over naked Yb_2TiO_5 which enhances separation of electron–hole pairs which improves antifungal activity.

Keywords Antifungal activity · Yb_2TiO_5@Ag nanocomposites · Optical properties

Introduction

In the recent years, application of nanomaterials has experienced a rapid growth thanks to introduce novel physical and chemical properties, especially semiconductor nanoparticles [1–3]. Fungi, kingdom of mostly microscopic organisms, can easily grow on the surface of materials and seriously threaten human health. Besides, in the third millennium, fungal diseases are an important cause of morbidity and mortality, especially in patients who suffer from having defect in their immune function. Candida, one of the famous fungal opportunistic pathogens, is specified as the part of human normal flora proliferates in gastrointestinal, genitourinary tracts, and oral cavity [4, 5]. Candida species are able to produce different types of diseases including local infection (skin and mucous) or disseminated infections which penetrate through the organs with the aid of blood stream [6, 7]. There are five impressive Candida species which cause more than 90% of invasive infections including *Candida albicans*, *Candida glabrata*, *Candida tropicalis*, *C. parapsilosis*, and *Candida krusei* [8]. In spite of various created antifungal drugs which commonly were used in clinical treatments, only a few number of drugs are attainable for candidiasis infections [9]. However, Candida species, especially non-albicans species such as *C. glabrata*, become resistant to antifungal agents which cause an increase in treatment failure [10]. Therefore, it is necessary to study the novel drugs which have less influenced on the fungal resistance mechanism. Nanotechnology recently developed many biocidal nanomaterials which demonstrated good antifungal activities against various fungi

✉ S. M. Hosseinpour Mashkani
seyedmostafa.hosseinpourmashkani@uts.edu.au

1 Department of Medical Parasitology and Mycology, Faculty of Medicine, Kashan University of Medical Sciences, Kashan, Iran

2 Infectious Diseases Research Center, Kashan University of Medical Sciences, Kashan, Iran

3 Institute for Biomedical Materials and Devices, School of Mathematical and Physical Sciences, Faculty of Science, University of Technology Sydney, Sydney, NSW 2007, Australia

4 Department of laboratory Science, Faculty of Para Medicine, Kashan University of Medical Science, Kashan, Iran

[11–15]. Many nanoparticles have been studied as antimicrobial agents, such as those of chitosan [16], MgO [17], silica-coated Fe_3O_4 [18], silver and its derivatives [19–21], TiO_2 [22], cobalt ferrite, and Fe_3O_4 [23, 24]. Ag compounds demonstrate having wide antimicrobial activities against bacteria, viruses, and fungi, with minimal development of microbial resistance. Antifungal and antibacterial properties of silver nanoparticles (AgNPs) originated from their ability for producing high levels of reactive oxygen species (ROS) and free radical species such as hydrogen peroxide, superoxide anion, hydroxyl radical, hypochlorous acid, and singlet oxygen [25–27]. In the absence of AgNPs, there is no substantial amount of ROS in cells and also it can be removed by antioxidant systems of the cell [28]. On the contrary, in the presence of AgNPs, they can inactivate dehydrogenases enzyme which causes an increase in ROS generation and consequently blocked respiration and growth of cells [29, 30]. On the other hand, AgNPs reduce producing level of antioxidant enzyme such as glutathione (GSH), superoxide dismutase, and catalase, which can accelerate the accumulation of ROS [31]. Eventually, accumulation of ROS causes apoptosis, lipid peroxidation, depletion of GSH, and DNA damage [32, 33]. The other thing is that AgNPs can release silver ions (Ag^+) [34–37], which are dependent on their surface area [38]. There are several possible mechanisms for the antifungal and antibacterial properties of silver ions. First of all, it can interface with sulfhydryl groups in enzymes and proteins. In other words, Ag ions can bind to proteins in the cell membrane and form stable bonds which cause to deactivate proteins which are included in transmembrane ATP generation and mediate ion transport across cell membranes [39]. Second of all, they can take place between the purine and pyrimidine base pairs and disrupt the H-bonds between base pairs of the anti-parallel DNA strands, which prevent cell division and reproduction eventually [40, 41]. Furthermore, Ag^+ as a heavy metal ion can cause cellular oxidative stress in microbes to increase. Herein, we applied simple two step sol-gel assistant ultrasonic method to synthesize YTi@Ag NPs in order to investigate its antifungal ability. The antifungal activities against Candida fungi group consisting of *C. albicans* (ATCC 1023), *C. krusei* (ATCC 6258), and *C. tropicalis* (ATCC 750) were investigated throughout the macrodilution method.

Experimental

Characterization

Materials and characterization: All chemical reagents in this experiment were of analytical grade and used without further purification, ytterbium salt, ethanol, silver nitrate, and tetra-n-butyl titanate (TNBT). X-ray diffraction (XRD) patterns were recorded by a Philips-X'Pert-Pro, X-ray diffractometer using Ni-filtered Cu Kα radiation at scan range of $10 < 2\theta < 80$. Scanning electron microscopy (SEM) images were obtained on LEO-1455VP equipped with an energy-dispersive X-ray spectroscopy. Fourier-transform infrared (FT-IR) spectra were recorded on Magna-IR, spectrometer 550 Nicolet with 0.125 cm^{-1} resolution in KBr pellets in the range of 400–4000 cm^{-1}. The EDS analysis with 20 kV accelerated voltage was done.

Synthesis of Yb_2TiO_5 nanocomposites

In a typical synthesis procedure, in two beakers, the stoichiometric amount (1:1) of tetra-n-butyl titanate (A) and ytterbium nitrate (B) was dissolved in ethanol, under stirring. Then, oxalic acid as a chelate agent was also dissolved in ethanol. Afterward, solutions A and B were mixed with the chelate agent solution under stirring at 90 °C for 30 min to form a gel. The final gel product was dried at 110 °C and then calcined at 800 °C for 3 h in a conventional furnace in air atmosphere.

Synthesis of YTi@Ag nanocomposites

In order to synthesize YTi@Ag nanocomposites, 0.5 g of as-synthesized Yb_2TiO_5 nanoparticles was dissolved in 20-ml ultra-pure water, while a 10 ml of silver nitrate solution (0.5 g) was added to it under stirring for 15 min. Afterward, above-mentioned solution was irradiated under ultrasonic probe, 180 W for 30 min. After irradiation, the system was allowed to cool to room temperature naturally, and the obtained precipitations were collected, washed three times with ethanol and distilled water, and dried under vacuum oven. It is worth mentioning that the electrostatic interaction (attraction) was happened between positive surface charge silver ions and negative surface charge Yb_2TiO_5 nanoparticles to make YTi@Ag nanocomposites.

Antifungal assay

The antifungal activity of YTi@Ag nanocomposites was performed according to the macrodilution method which is the recommended method by the Clinical and Laboratory Standards Institute (CLSI, document M27-A3). At first, YTi@Ag nanocomposites and Fluconazole were dissolved in distilled water and 100% dimethyl sulfoxide, respectively. Then, the above solutions were diluted, tenfold, by adding RPMI 1640 medium (with L-(3-N-morpholinepropanesulfonic acid). Afterward, 100 µl of aforementioned solutions was added into the wells micro-plate. It is noteworthy to mention that Fluconazole and YTi@Ag nanocomposites concentrations were 0.25–32 and 0.05–32 µg/ml, respectively. Then, three standard Candida species including *C.*

albicans (ATCC 1023), *C. krusei* (ATCC 6258), and *C. tropicalis* (ATCC 750) were sub-cultured on the Sabouraud dextrose agar and incubated at 35 °C for 24 h. After incubation, they were suspended in 5 ml of sterile water and shook vigorously. In order to obtain 0.5 McFarland standard (1×10^6 to 5×10^6 CFU/ml) turbidity, the turbidity was adjusted spectrophotometrically at 625 nm. The suspension was diluted (1:100) and followed (1:20 dilution) with RPMI 1640 medium to provide final concentration around $0.5–2.5\times10^3$ colony-forming units (c.f.u)/ml. Then, 900 µg/ml of the above-prepared concentration was added to each well. In order to have positive control, one well was just filled with 1000 µg/ml Candida suspension. Finally, the micro-plates incubated in incubator in a humid environment, at 35 °C for 48 h. The MIC^{50} which considers as the lowest drug concentration and could create a ≥ 50% reduction on fungal growth in compared to the drug-free growth control was determined visually after 24 and 48 h. The other thing is that inverted microscope was used to better viewing and remove turbidity problems originated from nanoparticles. The inhibition percentage (MIC^{50}) was calculated as follows (1):

$$\text{Inhabitation rate} = 1 - \left[\text{OD sample/OD control}\right] \times 100 \quad (1)$$

Results and discussion

Structural study

Figure 1a, b demonstrates the comparison of XRD patterns of Yb_2TiO_5 and YTi@Ag nanocomposites, respectively. Figure 1a shows cubic phase of YTi ($a=b=c=10.0300$ Å) with a space group of Fd-3m and JCPDS No. 33-1457. Furthermore, XRD pattern of YTi@Ag nanocomposites illustrates cubic phase of Yb_2TiO_5 (JCPDS No. 33-1457) along with cubic phase of Ag (JCPDS No. 87-0717 and space

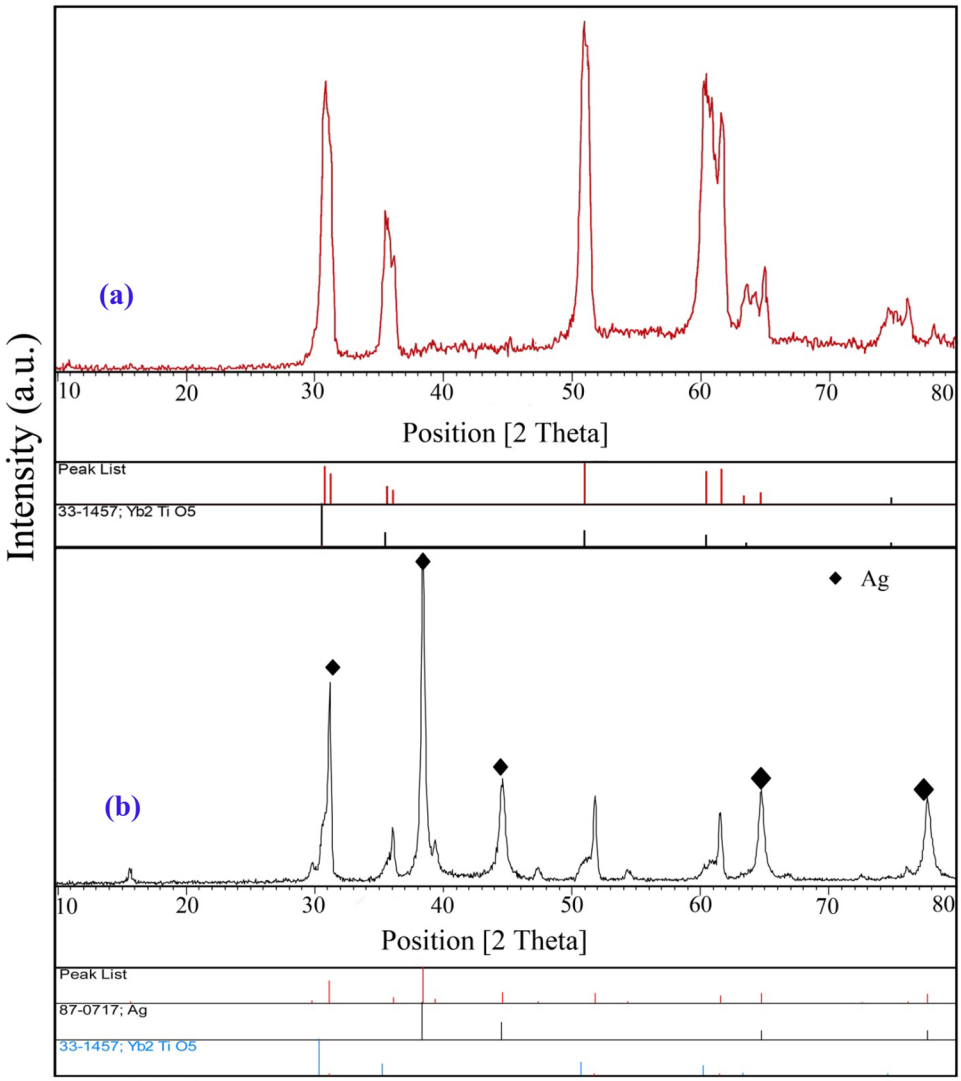

Fig. 1 XRD patterns of **a** Yb_2TiO_5 and **b** Yb_2TiO_5@Ag nanocomposites

group Fm-3m). No other crystalline phases are detected in the YTi@Ag nanocomposites. The crystallite diameter (D_c) of YTi@Ag nanocomposites (15.7 nm) was calculated through the Scherrer Eq. (2):

$$D_c = K\lambda/\beta\cos\theta \quad (2)$$

where β is the breadth of the observed diffraction line at its half intensity maximum, K is the so-called shape factor (0.9), and λ is the wavelength of X-ray source used in XRD. In order to further prove the chemical structure and composition of YTi@Ag nanocomposites, energy-dispersive spectroscopy (EDS) was performed, as shown in Fig. 2. Based on Fig. 2, nanocomposites consist of only Yb, Ti, O, and Ag atoms. FT-IR analysis was performed to confirm the presence of certain functional groups, as shown in Fig. 3. According to Fig. 3, the absorption bands at 3443 and 1633 cm^{-1} can be attributed to the stretching and bending vibrations of H_2O molecules that were absorbed on the surface of the nanoparticles [42]. The weak absorption peak at 594 cm^{-1} is attributed to the Ti–O bonds [3]. Moreover, an absorption peak at 491 cm^{-1} is assigned to Yb–O band. Scanning electron microscopy (SEM) was applied to demonstrate the morphology of YTi@Ag nanocomposites. Figure 4a, b shows the SEM images of Yb_2TiO_5 and YTi@Ag nanocomposites. Based on Fig. 4a, product mainly consists of homogenous nanoparticles, while adding Ag causes to somewhat increase the particles size and agglomeration of YTi@Ag (Fig. 4b). On the one hand, the surface charge of Yb_2TiO_5 is intrinsically negative due to the presence of five oxygen groups with negative charge. Therefore, Yb_2TiO_5 nanoparticles do not show aggregation or have very small amount of aggregation, due to the electrostatic repulsion between negative charges on their nanoparticles surface, as we can see in Fig. 4a. On the other hand, doping silver

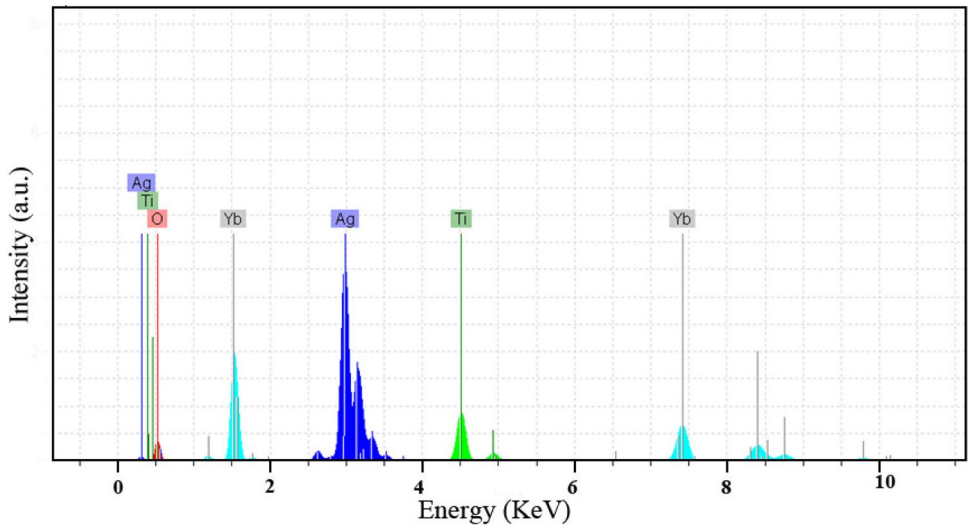

Fig. 2 EDS pattern of Yb_2TiO_5@Ag nanocomposites

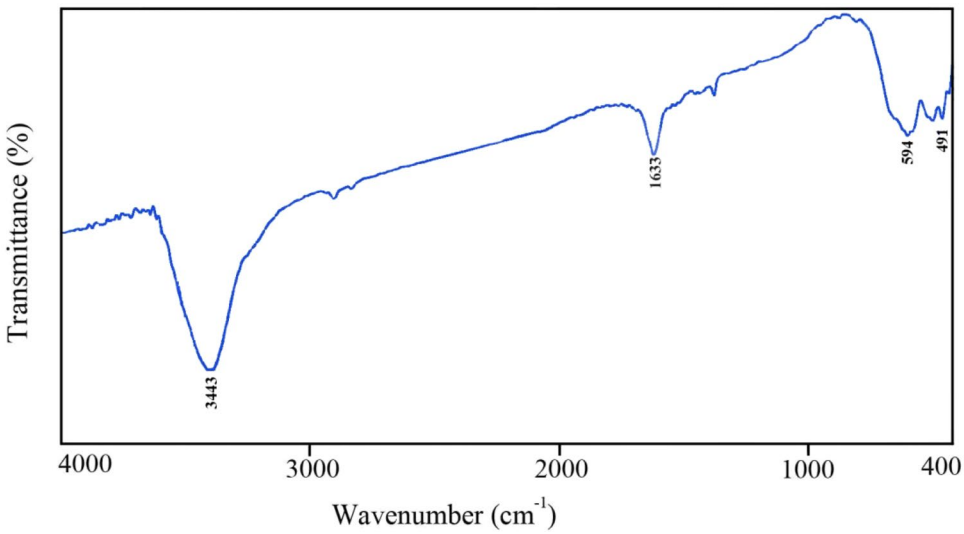

Fig. 3 FT-IR analysis of Yb_2TiO_5@Ag nanocomposites

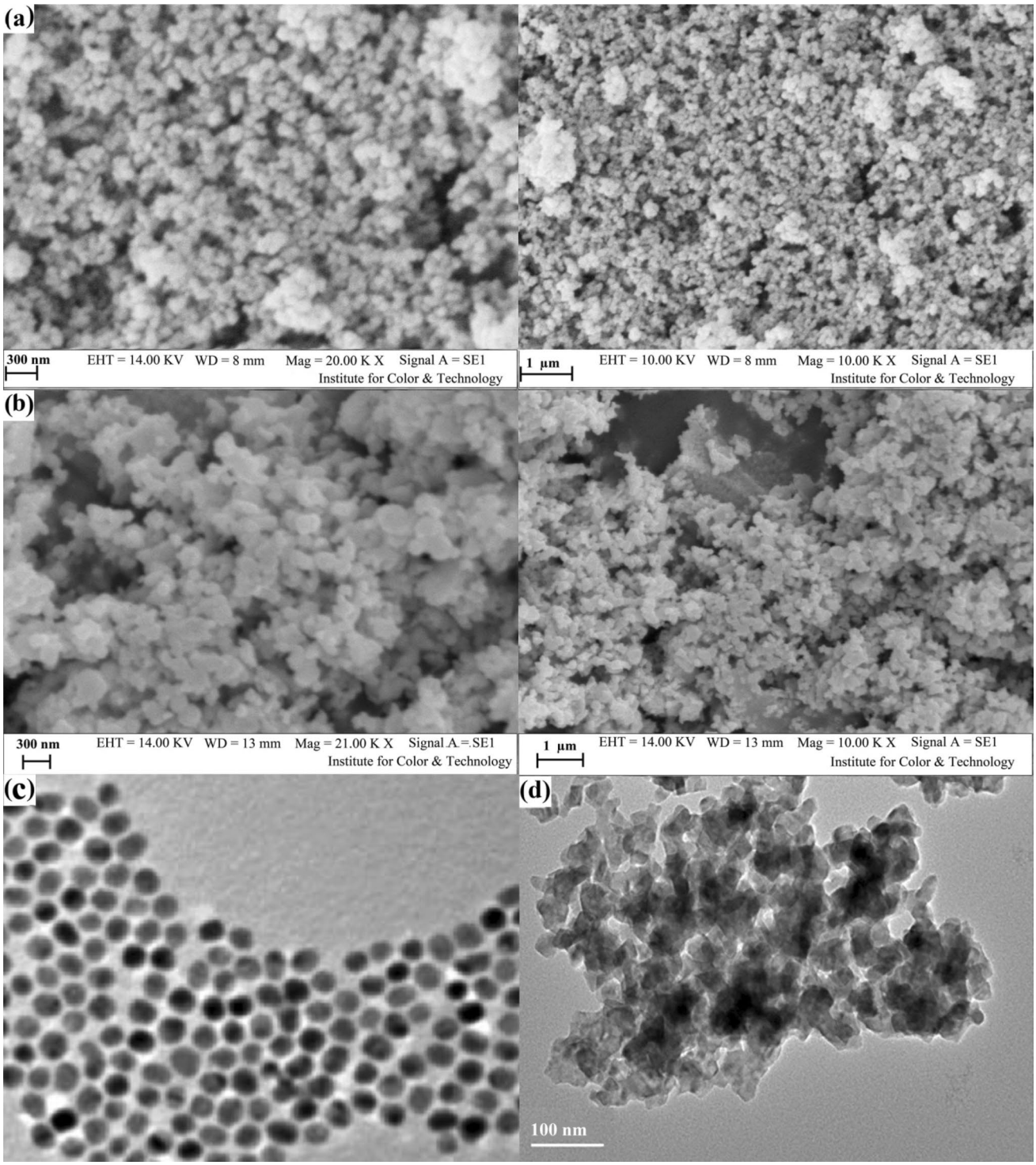

Fig. 4 **a**, **b** SEM images of Yb_2TiO_5 and Yb_2TiO_5@Ag nanocomposites. **c** TEM image of Yb_2TiO_5

nitrate creates aggregation because silver ions have positive charge and after mixing with Yb_2TiO_5 nanoparticles, which have negative surface charge, aggregates nanoparticles due to the electrostatic interaction between positive charge of silver ions and negative surface charge of Yb_2TiO_5 (Fig. 4b). TEM image of Yb_2TiO_5 (Fig. 4c) and YTi@Ag nanocomposites (Fig. 4d) is in agreement with their SEM images and confirms that adding Ag causes an increase in particle size along with agglomeration. Besides, TEM image of Yb_2TiO_5 consists of particles with average size 25–35 nm, while the

size of particles in nanocomposites is 45–60 nm. The optical properties of the as-synthesized Yb_2TiO_5 and YTi@Ag nanocomposites have been analyzed by UV–Visible spectroscopy, as shown in Fig. 5a, b, respectively. Based on the Tauc's relationship ($\alpha = \alpha_0(h\nu - E_g)n/h\nu$), E_g value decreased from 3 to 2.85 eV after doping Ag with Yb_2TiO_5 which is mainly due to the efficient substitution of Ag with ytterbium (Yb) atoms. The substitution process lowers the conduction band of the host material (Yb_2TiO_5) to more negative values. Moreover, surface oxygen vacancies and defect state may form because of doping that can capture the photoinduced electron during photocatalytic process, which can enhance photocatalytic inactivation of fungal. Therefore, silver-doped Yb_2TiO_5 is suitable candidate for enhancing antibacterial properties.

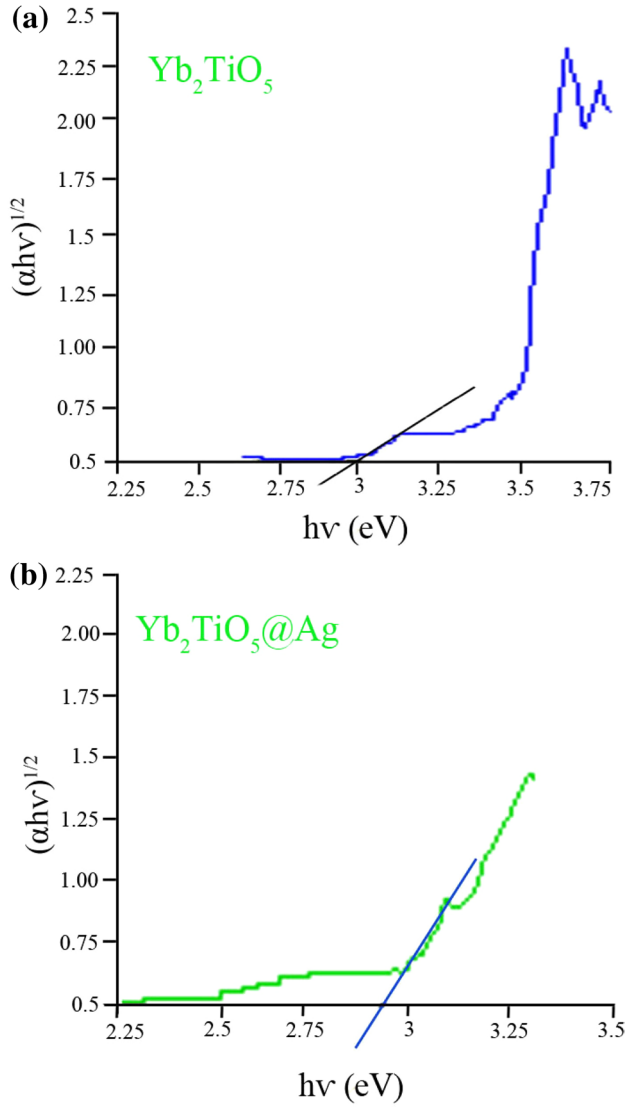

Fig. 5 UV–Vis spectra of **a** Yb_2TiO_5 and **b** Yb_2TiO_5@Ag nanocomposites

Antifungal assessment

A possible mechanism that could explain interaction between nanocomposite and antifungal is that YTi@Ag nanocomposites could utilize electrostatic interactions, hydrophobic effects, or van der Waals forces to be adsorbed on the cell membrane and release silver ions (Ag^+) and ROS. The as-released Ag^+ and ROS might have damaged the cell membrane throughout the mechanisms including protein coagulation, cell wall pits, inactivation of the respiratory chain, membrane permeability induction, and biosorption process [43]. YTi@Ag nanocomposites can benefit from the advantages of producing ROS by Yb_2TiO_5 along with realized silver ions (Ag^+) and ROS from YTi@Ag nanocomposites to demonstrate higher antifungal activity compared with pure silver nanoparticles. The antifungal activities of three different Candida species in the presence of YTi@Ag nanocomposites and Fluconazole (Fig. 6a, b, respectively) and silver nanoparticles for 24 and 48 h are listed in Table 1. Serial dilutions for YTi@Ag (1–8) wells were 32, 16, 4, 2, 1, 05, 0.25, and drug free, respectively. The one thing is

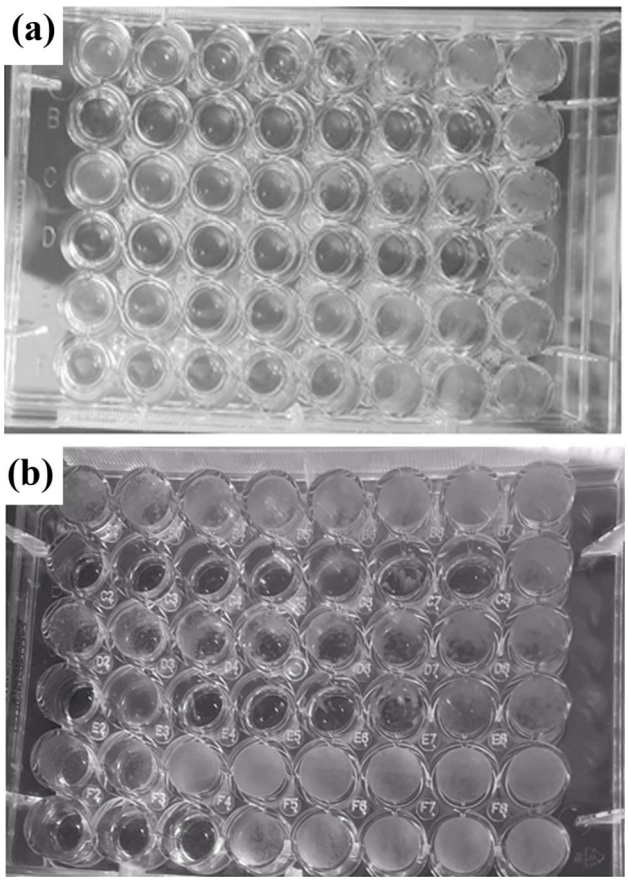

Fig. 6 Macrodilution assessment for MIC^{50} determination against Yb_2TiO_5@Ag (row A, C, and E) and Fluconazole (row B, D, and F) after 24 and 48 h

Table 1 MIC^{50} results of Yb_2TiO_5@Ag nanocomposites, Ag nanoparticles, and Fluconazole against three Candida species

Candida species	Fluconazole MIC^{50} µg/ml		Ag nanoparticles MIC^{50} µg/ml		Yb_2TiO_5@Ag MIC^{50} µg/ml	
Time	24 h	48 h	24 h	48 h	24 h	48 h
C. albicans (ATCC 1023)	0.25	0.5	3	20	4	32
C. tropicalis (ATCC 750)	0.25	1	2	17	4	32
C. krusei (ATCC 6258)	2	16	3.2	20	4	32

that, based on Table 1, MIC^{50} was significantly increased with increase in incubation time in the presence of YTi@Ag nanocomposites, while it was slightly increased in the presence of Fluconazole, except *C. krusei*. The other thing is that the MIC^{50} of YTi@Ag nanocomposites is higher than that of silver nanoparticles.

Conclusions

In summary, Yb_2TiO_5@Ag nanocomposites were synthesized through the sol-gel assistant ultrasonic method. Besides, various concentrations (0.25–32 and 0.05–32 µg/ml) of YTi@Ag nanocomposites were applied to investigate its antifungal activity against three standard Candida species including *C. albicans* (ATCC 1023), *C. krusei* (ATCC 6258), and *C. tropicalis* (ATCC 750) in comparison with Fluconazole. Antifungal results demonstrate that maximum MIC^{50} for three standard Candida species was 4 and 32 µg/ml after 24 and 48 h, respectively. In addition, MIC^{50} value of Yb_2TiO_5@Ag nanocomposites is higher than pure silver nanoparticles due to the synergetic effect of Ag^+ and ROS in nanocomposite.

Acknowledgements This study financial supported by research project (98105) of Kashan University of Medical sciences and Health Services.

Compliance with ethical standards

Conflict of interest The authors declare that they have no conflict of interest.

References

1. S.M. Hosseinpour-Mashkani, A. Sadeghinia, Z. Zarghami, K. Motevalli, J. Mater. Sci. Mater. Electron. **27**, 365 (2016)
2. M. Mansournia, S. Rafizadeh, S.M. Hosseinpour-Mashkani, J. Mater. Sci. Mater. Electron. **26**, 5839 (2015)
3. S.M. Hosseinpour-Mashkani, M. Maddahfar, A. Sadeghinia, M. Ramezani, J. Mater. Sci. Mater. Electron. **26**, 3359 (2015)
4. J.D.C.O. Sardi, D.R. Silva, M.J.S. Mendes-Giannini, P.L. Rosalen, Microb. Pathog. **125**, 116 (2018)
5. L.A.N. Egue, J.P.K.M. Bouatenin, F.K. Nguessan, M. Koussemon-Camara, Microb. Pathog **124**, 5 (2018)
6. R. López-Martínez, Clin. Dermatol. **28**(2), 178 (2010)
7. D. Kontoyiannis, E. Mantadakis, G. Samonis, J. Hosp. Infect. **53**(4), 243 (2003)
8. D.M. MacCallum, Int. J. Microbiol. **2012**, 363764 (2011)
9. B.P. Mathew, M. Nath, Chem. Med. Chem. **4**(3), 310 (2009)
10. R. Razzaghi, M. Momen-Heravi, M. Erami, M. Nazeri, Curr. Med. Mycol. **2**(3), 20 (2016)
11. G. Li, H. Zhao, J. Hong, K. Quan, Q. Yuan, X. Wang, Colloids Surf. B **160**, 220 (2017)
12. S. Gowri, R. Rajiv Gandhi, M. Sundrarajan, J. Mater. Sci. Technol **30**, 782 (2014)
13. A.S.H. Hameed, C. Karthikeyan, V.S. Kumar, S. Kumaresan, S. Sasikumar, Mater. Sci. Eng. C **52**, 171 (2015)
14. P. Balashanmugam, M.D. Balakumaran, R. Murugan, K. Dhanapal, P.T. Kalaichelvan, Microbiol. Res. **192**, 52 (2016)
15. D. Sharma, J. Rajput, B.S. Kaith, M. Kaur, S. Sharma, Thin Solid Films **519**, 1224 (2010)
16. G. Fiorani, O. Saoncella, P. Kaner, S.A. Altinkaya, A. Figoli, M. Bonchio, M. Carraro, J. Clust. Sci. **25**, 83 (2014)
17. H. Beyzaei, R. Aryan, H. Molashahi, M.M. Zahedi, A. Samzadeh-Kermani, B. Ghasemi, M. Moghaddam-Manesh, J. Iran. Chem. Soc. **14**, 1023 (2017)
18. D. Azarifar, H. Ebrahimiasl, R. Karamian, M. Ahmadi-Khoei, J. Iran. Chem. Soc. **16**, 341 (2019)
19. M.A. Azeez, A. Lateef, T.B. Asafa, T.A. Yekeen, A. Akinboro, I.C. Oladipo, E.B. Gueguim-Kana, L.S. Beukes, J. Clust. Sci. **28**, 149 (2017)
20. P. Karthiga, S. Rajeshkumar, G. Annadurai, J. Clust. Sci. **29**, 1233 (2018)
21. E.E. Elemike, D.C. Onwudiwe, O.E. Fayemi, A.C. Ekennia, E.E. Ebenso, L.R. Tiedt, J. Clust. Sci. **28**, 309 (2017)
22. M. Ghanbari-Mehrabani, R. Karimian, R. Rakhshaei, F. Pakdel, H. Eslami, V. Fakhrzadeh, M. Rahimi, R. Salehi, H. Samadi-Kafil, Int. J. Biol. Macromol. **116**, 966 (2018)
23. A.A. Agale, S.M. Janjal, S.T. Gaikwad, A.S. Rajbhoj, J. Clust. Sci. **28**, 477 (2017)
24. P.M. Anjana, M.R. Bindhu, M. Umadevi, R.B. Rakhi, J. Mater. Sci. Mater. Electron. **29**, 6040 (2018)
25. R. Zhao, M. Lv, Y. Li, M. Sun, W. Kong, L. Wang, S. Song, C. Fan, L. Jia, S. Qiu, Y. Sun, H. Song, R. Hao, ACS Appl. Mater. Interfaces **9**(18), 15328 (2017)
26. E.Z. Gomaa, J. Gen. Appl. Microbiol. **63**(1), 36 (2017)
27. P. Siritongsuk, N. Hongsing, S. Thammawithan, S. Daduang, S. Klaynongsruang, A. Tuanyok, R. Patramanon, PLoS ONE **11**(12), e0168098 (2016)
28. B. Ramalingam, T. Parandhaman, S.K. Das, ACS Appl. Mater. Interfaces **8**(7), 4963 (2016)
29. M.A. Quinteros, V. Cano Aristizábal, P.R. Dalmasso, M.G. Paraje, P.L. Páez, Toxicol In Vitro **36**, 216 (2016)
30. H.L. Su, C.C. Chou, D.J. Hung, S.H. Lin, I.C. Pao, J.H. Lin, F.L. Huang, R.X. Dong, J.J. Lin, Biomaterials **30**(30), 5979 (2009)
31. Y.G. Yuan, Q.L. Peng, S. Gurunathan, Int. J. Mol. Sci. **18**(3), 569 (2017)
32. P. Korshed, L. Li, Z. Liu, T. Wang, PLoS ONE **11**(8), e0160078 (2016)

33. W. Lee, K.J. Kim, D.G. Lee, Biometals **27**(6), 1191 (2014)
34. X. Zhong, Y. Song, P. Yang, Y. Wang, S. Jiang, X. Zhang, Changyi Li. PLoS ONE **11**(1), e0146957 (2016)
35. J.C. Jin, X.J. Wu, J. Xu, B.B. Wang, F.L. Jiang, Y. Liu, Biomater. Sci. **5**(2), 247 (2017)
36. P.C. Lombardo, A.L. Poli, L.F. Castro, J.R. Perussi, C.C. Schmitt, ACS Appl. Mater. Interfaces **8**(33), 21640 (2016)
37. T. Kim, G.B. Braun, Z.G. She, S. Hussain, E. Rouslahti, M.J. Sailor, ACS Appl. Mater. Interfaces **8**(44), 30449 (2016)
38. K. Zawadzka, K. Kądzioła, A. Felczak, N. Wrońska, I. Piwoński, A. Kisielewska, K. Lisowska, New J. Chem. **38**(7), 3275 (2014)
39. U. Klueh, V. Wagner, S. Kelly, A. Johnson, J.D. Bryers, J. Biomed. Mater. Res. **53**(6), 621 (2000)
40. D.W. Hatchett, H.S. White, J. Phys. Chem. **100**(23), 9854 (1996)
41. D.R. Monteiro, L.F. Gorup, A.S. Takamiya, E.R. de Camargo, A.C. Filho, D.B. Barbosa, J. Prosthodont. **21**(1), 7 (2012)
42. A. Javidan, S. Rafizadeh, S.M. Hosseinpour-Mashkani, Mater. Sci. Semicond. Process. **27**, 468 (2014)
43. Z. Kanwal, M. Akram Raza, S. Riaz, S. Manzoor, A. Tayyeb, I. Sajid, S. Naseem, R. Soc. Open Sci. **6**(5), 182135 (2019)